EFDA–JET–PR(10)34

X. Litaudon, Y. Sakamoto, P.C. de Vries, A. Salmi, T. Tala, C. Angioni, S. Benkadda, M.N.A. Beurskens, C. Bourdelle, M. Brix, K. Crombé, T. Fujita, S. Futatani, X. Garbet, C. Giroud, N.C. Hawkes, N. Hayashi, G.T. Hoang, D. Hogeweij, G. Matsunaga, T. Nakano, N. Oyama, V. Parail, K. Shinohara, T. Suzuki, M. Takechi, H. Takenaga, T. Takizuka, H. Urano, I. Voitsekhovitch, M. Yoshida, ITPA Transport Group, the JT-60 team and JET EFDA contributors

Core Transport Properties in JT-60U and JET Identity Plasmas

Core Transport Properties in JT-60U and JET Identity Plasmas

X. Litaudon[1], Y. Sakamoto[2], P.C. de Vries[3], A. Salmi[4], T. Tala[5], C. Angioni[6], S. Benkadda[7], M.N.A. Beurskens[8], C. Bourdelle[1], M. Brix[8], K. Crombé[9], T. Fujita[2], S. Futatani[1], X. Garbet[1], C. Giroud[8], N.C. Hawkes[8], N. Hayashi[2], G.T. Hoang[1], D. Hogeweij[3], G. Matsunaga[2], T. Nakano[2], N. Oyama[2], V. Parail[8], K. Shinohara[2], T. Suzuki[2], M. Takechi[2], H. Takenaga[2], T. Takizuka[2], H. Urano[2], I. Voitsekhovitch[8], M. Yoshida[2], ITPA Transport Group, the JT-60 team[10] and JET EFDA contributors*

JET-EFDA, Culham Science Centre, OX14 3DB, Abingdon, UK

[1]CEA, IRFM, F-13108 St-Paul-Lez-Durance, France
[2]Japan Atomic Energy Agency, Naka, Ibaraki-ken, 311-0193, Japan
[3]FOM institute Rijnhuizen, EURATOM association, 3430BE, Nieuwegein, Netherlands
[4]Association Euratom-Tekes, Helsinki University of Technology, P.O. Box 4100, Finland
[5]Association Euratom-Tekes, VTT, PO Box 1000, 02044 VTT, Finland
[6]Max-Planck-Institut für Plasmaphysik, Euratom Association, 85748 Garching, Germany
[7]International Institute for Fusion Science, CNRS-Université de Provence, Marseille, France
[8]EURATOM-CCFE Fusion Association, Culham Science Centre, OX14 3DB, Abingdon, OXON, UK
[9]Department of Applied Physics, Ghent University, Rozier 44, 9000 Gent, Belgium
[10]See annex of N. Oyama Nuclear Fusion 49
** See annex of F. Romanelli et al, "Overview of JET Results", (23rd IAEA Fusion Energy Conference, Daejon, Republic of Korea (2010)).*

Preprint of Paper to be submitted for publication in
Nuclear Fusion

ABSTRACT.
The paper compares the transport properties of a set of dimensionless identity experiments performed between JET and JT-60U in the advanced tokamak regime with Internal Transport Barrier, ITB. These International Tokamak Physics Activity, ITPA, joint experiments were carried out with the same plasma shape, toroidal magnetic field ripple and dimensionless profiles. Similarities in the ITB triggering mechanisms and sustainment were observed when a good match was achieved of the most relevant normalized profiles except the toroidal Mach number. Similar thermal ion transport levels have been measured in either monotonic or non-monotonic q-profiles. On the contrary, differences between JET and JT-60U were observed on the electron thermal and particle confinement in reversed magnetic shear configurations. The large shear reversal in the center of JT-60U plasmas allowed the sustainment of stronger electron density ITBs compared to JET. As a consequence of peaked density profile, the core bootstrap current density is more than five times higher in JT-60U compared to JET and reversed magnetic shear configurations are self-sustained in JT-60U scenarios.

1. INTRODUCTION

Steady-state operation in ITER is foreseen to be with 100% non-inductive current drive at moderate plasma current (I_p~9MA) with Q_{DT}~5 for a burning time of 3000s. Efficient steady-state operation should be compatible with a large fraction of off-axis current provided by the bootstrap effect. The rest of the current is driven with non-inductive current drive sources. To compensate for the reduction of confinement due to a lower current, steady-state operation requires the confinement to be improved beyond that achieved with an edge transport barrier, up to $H_{IPB98(y,2)}$~1.5. A possible solution consists in optimizing the core confinement with an Internal Transport Barrier, ITB [1]. The predictive modelling of ITER steady-state scenario relies on a better understanding of the underlying ITBs physics. The purpose of the paper is to improve our understanding of the core confinement by comparing the transport properties in a set of identity experiments [2] performed between JT-60U and JET in the ITB regime [3-4]. The results obtained in the advanced regime extend past identity JET and JT-60U experiments in inductive H-mode scenario [5]. In these recent experiments, the key challenge was in matching not only the 0-D global parameters but the full 1-D radial profiles of the normalised physics parameters that govern the plasma properties. In section 2, the operational scenario to match the normalised physics quantities between JET and JT-60U is briefly summarised. In section 3, the modelling approach to quantitatively assess the transport properties of the two devices is described. Then, emphasis is given on the transport analysis during the ITB phase by comparing thermal coefficients and electron particle diffusivities in weak and reversed magnetic shear plasmas. To conclude, an explanation is proposed in section 4 to throw light on the subtle differences in the electron density profiles observed between the two devices. Consequences of the transport analysis for the operational scenario are also given.

2. DESCRIPTION OF THE JT-60U AND JET OPERATIONAL SCENARIO

Similar operational scenarios were developed in the two devices with the objective of triggering

the ITBs during the plasma current flat top phase where neutral beam injection, NBI, power only was applied in conditions with identical magnetic configurations (Fig.1). The 0-D parameters are listed in table 1 and have been chosen to match the 0-D normalised physics quantities. In the JET experiments the Toroidal magnetic Field (TF) ripple, δ_{TF}, which is known to affect the particle transport properties, rotation and ITB characteristics [6], was changed, from the standard value of $\delta_{TF} = 0.08\%$ at the mid-plane of the outer separatrix, to higher values matching the TF ripple in JT-60U, $\delta_{TF} = 0.3\%$, and even up to $\delta_{TF} = 0.75\%$. In JT-60U, the toroidal torque on the plasma was tuned by applying different amounts of co- and counter-current NBI power fractions. Finally, to match and vary the current density profiles in the two devices, NBI heating in JT-60U and Lower Hybrid Current Drive powers in JET are used during the ramp up phase. Similar safety factor, q, profiles were obtained (Fig.1) with either, low positive magnetic shear and $q_o \sim 2$ in the centre, or, negative and reversed magnetic shear in the core (and a minimum q, $q_{min} \sim 3$ or 2 located at mid-plasma radius). Identity experiments were performed by tuning the power level, the timing of the high power phase, the NBI set-up and density in the prelude phase. Consequently, JET and JT-60U experiments were carried out with the same plasma shape and dimensionless profiles: safety factor, normalized Larmor radius, normalized collision frequency, thermal beta, ratio of ion to electron temperatures etc. Similarities of the ITB triggering mechanism and the ITB strength have been observed when a proper match is achieved of the relevant profiles of the normalized quantities [3-4]. The paper focuses on the fully developed ITBs characteristics and transport properties in plasmas with different q-profiles and magnetic shears ranging from negative to positive values in the plasma core.

3. TRANSPORT PROPERTIES IN WEAK AND REVERSED MAGNETIC SHEAR CONFIGURATIONS

Core transport properties are investigated using the same methodology, similar measurements, and the same set of codes for both devices. In order to carry out a transport analysis, detailed plasma profiles measurements and source terms calculation are required. The safety factor is constrained with combined 0-D magnetic data and MSE measurements. The ion temperature, T_i, and toroidal rotation, V_ϕ, profiles of the ionised carbon impurity are measured by Charge Exchange Spectroscopy in JET and JT-60U. The electron density and temperatures are measured with the Thomson scattering diagnostics. NBI heating, fuelling, torque and current drive sources are calculated using the guiding centre following Monte-Carlo ASCOT code that takes into account the fast ion ripple loss effect [7]. The effect of TF- ripple on the source terms has to be included in the calculation since its magnitude will impact the fast particle confinement. For each JET and JT-60U discharge, specific times have been selected corresponding to the ITB triggering and fully developed phases. At each time, the 2-D magnetic equilibrium, the fitted 1-D radial plasma profiles are used as an input to the ASCOT-code to evaluate the NBI source terms. Then, the NBI sources computed by ASCOT are coupled to the transport code JETTO to calculate the neo-classical quantities from NCLASS [8], the thermal heat and electron particle diffusivities. Typical results of ASCOT are shown on Fig.2

(right) where the NBI sources have been calculated in reversed shear ($q_{min} = 2$) for three levels of TF-ripple in JET and three levels of injected torque in JT-60U. The calculations confirmed that the NBI power is mainly deposited on the thermal ions in the two machines. Due to the differences in NBI configuration (Fig.2 (left)), the profiles of NBI fuelling, heating and torque sources are slightly broader in JT-60U compared to JET. The injected torque at the outer part of the plasma column ($\rho \sim 0.6$-1) is similar between JET and JT-60U when the JET TF ripple magnitude is increased to be in the range of 0.3-0.75%.

The evaluation of the non-dimensional 1-D profiles as the normalised thermal energy btor, normalised gyro-radius, $\rho_{e,i}$*, collisionality, ν_e*, normalised toroidal rotation, MF, is crucial for comparing the JET and JT-60U regimes since they determine the behaviour of the key physics processes. Similar calculation for JET and JT-60U has been done to estimate the dimensionless quantities from the measured thermal radial profiles.

3.1. WEAK MAGNETIC SHEAR PLASMAS IN JT-60U AND JET

Identity experiments were first performed with monotonic q-profiles. Very similar ITB phenomenology was observed between the two devices when matching, at the time of the ITB formation the following profiles: q, $\beta_{tor\text{-}e,i}$, ν_e*, $\rho_{e,i}$* for the same plasma shape and the same TF-ripple magnitude (0.3%). Due to the differences in NBI injected torque, the toroidal Mach numbers are different in the two devices. During the high performance phase with a fully developed ITB, similar normalised profiles were also obtained (except for the Mach number) as shown on Fig.3. In the two machines, the ion temperature profiles gradually increase from the ITB foot to the plasma center with a normalised ion temperature gradient scale length, R/L_{Ti} above 16. The electron temperature and the electron density profiles are also similar with $R/L_{Te} \sim 10$ and the density gradient scale length, $R/L_{ne} \sim 8$. Similar thermal ion transport level (normalised to gyro-Bohm level) between JET and JT-60U is computed with $\chi_i/\chi_{gyro\text{-}Bohm} \sim 0.1$ inside the ITB and $\chi_i/\chi_{gyro\text{-}Bohm} \sim 2$ at the ITB foot.

3.2. REVERSED MAGNETIC SHEAR PLASMAS IN JT-60U AND JET

For the reversed shear configurations, experimental effort focused on obtaining similar values of qmin, at the same radial location. Consequently, the q-profiles are very well matched between the two devices down to a normalized radius of $\rho \sim 0.2$-0.3 as shown on Fig.4 (left) and 5 (left) with $q_{min} \sim 2$ at mid plasma radius. In the very core (inside $\rho < 0.25$), JT-60U plasmas have much higher values of q_o (with $q_o > 6$) presenting the characteristics of a "current-hole" magnetic configuration that is sustained during the high power phase. Whereas in JET, the 'current hole' formed in the low density ramp-up phase with LHCD is rapidly filled by on-axis current when NBI power is applied leading to $q_o \sim 3$. In reversed shear configurations, a TF and a torque scan have been performed on JET and JT-60U respectively. The measured profiles and dimensionless quantities are shown on Fig's.4, 5 and 6. T_i-ITB characteristics (ITB position, R/L_{Ti} at the ITB foot) are very similar with normalised thermal ion transport levels between JET and JT-60U: $\chi_i/\chi_{gyro\text{-}Bohm} \sim 1$ at the ITB foot, and, $\chi_i/\chi_{gyro\text{-}Bohm} \sim 0.1$ inside the ITB (Fig. 6(left)). The reduction of the toroidal rotation is clearly

observed on the angular or Mach profiles for the highest TF-ripple value (Fig.4, 5). A value of $\delta_{TF} = 0.75\%$ is required on JET to match the evanescent toroidal rotation or the low Mach number for $\rho > 0.6$ as measured on JT-60U (Fig.4, 5). The increase of TF-ripple up $\delta_{TF} = 0.75\%$ affects the toroidal rotation but not the characteristics of the thermal ITB. These results complement previous JET observations where a larger TF-ripple scan was performed [6]. In the plasma core, the toroidal rotation and the Mach number are typically a factor two higher on JET compared to JT-60U as a consequence of higher injected torque on JET. During the JT-60U torque scan, the toroidal rotation profiles keep the same shape but are shifted in amplitude whereas n_e, T_i and, T_e profiles are practically unchanged. As in the weak shear case, the location of the ITB foot on the toroidal rotation is more inward ($\rho \sim 0.4$) compared to the one T_i ($\rho \sim 0.6$). The variation of toroidal rotation within the experimental range available, does not lead to significant variation of ion/electron thermal transport properties.

Contrary to the weak shear configuration, significant differences between JET and JT-60U are observed in reversed shear scenarios for the electron transport. Peaked electron density profiles are measured in JT-60U despite a broader fuelling source (Fig.2 (right)) with a peaking coefficient and a core density higher by nearly a factor two compared to JET, while the electron temperatures are similar in the two devices (Fig.4-5). In JT-60U, the electron density profile increases with nearly a constant slope from the ITB foot up to the plasma core. Whereas on JET, the steep density profiles (with $R/L_{ne} \sim$ 8-12) is well localised at the ITB foot in a narrow radial layer between $\rho \sim 0.4$-0.5. Outside, this layer the normalised density gradient length is significantly reduced with R/L_{ne} below 2. The calculated electron diffusivities, $\chi_e/\chi_{gyro\text{-}Bohm}$, decrease continuously in JT-60U core (below $\sim$ 0.1) whereas in JET electron diffusivities are locally reduced down to $\chi_e/\chi_{gyro\text{-}Bohm} \sim 0.1$ in a narrow radial layer located around qmin. Effective electron particle diffusion coefficients, D_{eff}, have also been estimated assuming that the NBI fuelling is the only particle source in the core. Edge fuelling from cold neutrals particles (wall recycling) is found negligible in the plasma core with respect to NBI fuelling: cold neutrals do not penetrate beyond the pedestal. In stationary conditions, D_{eff} is calculated as the ratio of the NBI fuelling source to the density gradient. As observed for the electron thermal diffusivities profiles, Deff decreases continuously in JT-60U (from $D_{eff}/\chi_{gyro\text{-}Bohm} \sim 1$ down to $D_{eff}/\chi_{gyro\text{-}Bohm} \sim 0.01$) whereas in JET D_{eff} coefficients are reduced (down to $D_{eff}/\chi_{gyro\text{-}Bohm} \sim 0.01$) but only in a narrow radial layer located around q_{min}.

DISCUSSION AND CONCLUSION

In order to explain the strong density peaking in JT-60U and the differences with JET, various physics interpretations are reviewed in this section. The difference between the two machines cannot be explained by the difference in core fuelling, on the contrary, the core fuelling is higher on JET with lower core density. A second interpretation based on the differences in neo-classical convective velocity is also not sufficient. Indeed, the Ware's pinch velocity is small in these non-inductive regimes: less than 0.05m/s.

The physical process producing electron particle transport in the core of tokamak plasma has

been recently reviewed in inductive operation with monotonic q-profile [9]. In low collisionality H-mode regime, the electron density peaking results from core turbulence producing non-diagonal contribution to the particle flux [10]. In the non-inductive ITB regimes, two complementary interpretations are investigated in this paper. These interpretations rely on core fuelling with either (i) a quench of the anomalous turbulence leading to a reduction of D_{eff} in the negative magnetic shear region or (ii) a reduction of D_{eff} combined with an inward (turbulence driven) convective electron particle flux.

The possibility to quench the turbulence at wavelength of the order of the ion Larmor radius scale length ($k_\perp \rho_i \sim 1$), i.e. the ion temperature gradients, ITG, modes and the trapped electron mode, TEM, has been checked using the QuaLiKiz code [11-12]. The QuaLiKiz calculation of the turbulent energy and particle fluxes is based on gyrokinetic quasi-linear assumptions [11-12]. The experimental profiles have been used has an input to QuaLiKiz simulations to calculate the linear ITG/TEM growth rates, $\gamma_{ITG\text{-}TEM}$, for $k_\perp \rho_i < 2$. The radial electric field E×B shearing rates, $\gamma_{E\times B}$, have been also calculated using the experimental pressure and toroidal rotation profiles but assuming a neo-classical poloidal rotation. Reversed shear discharges with $q_{min} \sim 2$ have been selected for JET and JT-60U (Fig.7 (left)). The QuaLiKiz calculations illustrate the stabilizing impact of the magnetic shear reversal in the core of the JT-60U discharge. The JET discharge has been selected with large TF-ripple amplitude $\delta_{TF} = 0.75\%$ to match the JT-60U toroidal rotation measured in the Pulse No: 49469 outside the ITB radius. Within the neo-classical assumption for the poloidal rotation, the radial electric field is dominated by the toroidal rotation term which explains why the maximum ExB shearing rate is a factor two larger in JET compared to JT-60U. Similar values of $\gamma_{ITG\text{-}TEM} \sim 0.15$MHz for JET and JT-60U have been found at the ITB foot ($\rho \sim 0.5$). On both devices, the difference in radial location of the maximum values of $\gamma_{ITG\text{-}TEM}$ and $\gamma_{E\times B}$ is explained by the difference in the location of the ITB foot on the rotation and thermal ion profiles. On JET, the ITG/TEM turbulences are not fully stabilised with $\gamma_{lin} \sim 0.05$MHz at $\rho \sim 0.4$: a value comparable to the maximum values of E×B shearing rates. On JT-60U core, the TEM and ITG modes are stabilised up to $\rho \sim 0.45$ due to the combined effect of the shear reversal and density peaking without necessarily invoking the E×B shearing rate stabilisation.

When neglecting the convective effects, the calculated low D_{eff} values lead to a ratio of electron particle to thermal transport, D_{eff}/χ_e, lower than 1/6 which is not theoretically justified in the low $k_\perp \rho_i$ turbulence regime. For an electrostatic turbulence in a tokamak, it has been found that the ratio of the diffusion coefficient to heat conductivity should be $\sim 2/3$ [13]. The remaining electron temperature gradient, ETG, driven turbulence at $k_\perp \rho_i > 1$ is a possible candidate to explain the larger heat transport than the particle transport or anomalous particle convective terms have to be invoked.

To investigate the turbulent convective terms, the first analysis involves a numerical solution of the non-linear fluid equations of ITG/TEM electrostatic turbulence in the collisionless regime using the TRB code [14]. Two sets of simulations have been carried out by changing the q-profile in the core from weakly to strongly reversed shear. TRB could reproduce the experimental trends thanks to the effect of an inward thermodiffusion pinch driven by the remaining ITG turbulence,

but at the expense of assuming a ratio of the ion to the electron heat sources, $S_i/S_e \sim 0.3$ (much lower than the experimental case where $S_i/S_e \sim 4$).

The second analysis relies on gyrokinetic quasi-linear calculation with QuaLiKiz. Four simulations have been considered (Fig.7 (right)): (1) the weak shear discharge (JT-60U Pulse No: 49476); (2) the same case as (1) but $\nabla T_e/T_e$ is increased by a factor two; (3) the same case as (1) but the q-profile is taken from the reversed shear discharge (JT-60U Pulse No: 49469); (4) the reversed shear discharge (JT-60U Pulse No: 49469). In case 1, the coexistence of ITG/TEM mode leads to an outward convective term in the core ($\rho < 0.4$). Indeed, the inward thermodiffusion particle pinch driven by ITG is compensated by the outward pinch induced by the dominant electron TEM turbulence (the compressibility pinch is small). The outward thermodiffusion convection velocity is reinforced when $|\nabla T_e/T_e|$ is increased by a factor two (case 2). TEM instabilities are reduced when changing only the q-profile from weak to reversed shear (with the thermal profiles of the weak shear case). The core thermodiffusion and the anomalous velocities switch their sign from outward to inward inside $\rho < 0.4$ (case 3). Finally, when including the density peaking effect (case 4), the ITG modes are fully stabilised.

This is a virtuous stabilisation circle where the stabilisation of the TEM modes by shear reversal leads to an inward convection and peaked electron density profile. The density gradient is then able to further stabilise the remaining ITG turbulence leading to a stronger reduction of the particle transport. Differences in electron pressure gradients, lead to significant differences in the core bootstrap and in the q-profiles that are non-linearly coupled to the plasma transport properties. The subtle differences in transport lead to a bifurcation of the final plasma state as observed with the JET and JT-60U reversed shear plasmas.

ACKNOWLEDGEMENT

This work, supported by the European Communities under the contract of Association between EURATOM and CEA, was carried out within the framework of the European Fusion Development Agreement. The views and opinions expressed herein do not necessarily reflect those of the European Commission. The experiments were performed in the framework of the ITPA and IEA Large Tokamak Cooperation collaborative activities.

REFERENCES

[1]. Connor J.W. et al., Nuclear Fusion **44** (2004) R1
[2]. Luce T.C. et al., Nuclear Fusion **43** (2003) 321
[3]. De Vries P.C. et al., Plasma Physics and Controlled Fusion **51** (2009) 124050
[4]. Sakamoto Y. et al., 12th International Workshop on "H-mode Physics and Transport Barriers" Sep. 30-Oct. 2, 2009 Princeton University, Plasma Physics Laboratory
[5]. Saibene G. et al., Nucl. Fusion **47** (2007) 969
[6]. De Vries P.C. et al., Plasma Physics and Controlled Fusion **50** (2008) 065008
[7]. Salmi A. et al. Contributions to Plasma Physics **48** (2008) 77

[8]. Houlberg W A et al., Physics of Plasmas **4** (1997) 3230
[9]. Angioni C. et al., Plasma Physics and Controlled Fusion **51** (2009) 124017
[10]. Angioni C. et al., Physical Review Letters **90** (2003) 205003
[11]. Bourdelle C. et al., Physics of Plasmas 14 (2007) 112501
[12]. Casati A. et al Nuclear Fusion **49** (2009) 085012
[13]. Garbet X. et al., Physics of Plasmas **12** (2005) 082511
[14]. Garbet X. et al., Physical Review Letters **91** (2003) 035001-1

	JET	**JT-60U**
$\mathbf{R_o}$ **(m)**	3.1	3.3
a (m)	0.9	0.8
R/a	3.45	4.13
k	1.62	1.60
δ	0.22	0.23
$\mathbf{B_o}$ **(T)**	2.3	2.3
$\mathbf{I_p}$ **(MA)**	1.5	1.1
$\mathbf{q_{95}}$	4.2	4.2
$\mathbf{\delta_{TF}}$ **(%)**	0.08, 0.3, 0.75	0.3

Table 1: 0-D parameters of JET and JT-60U identity experiments.

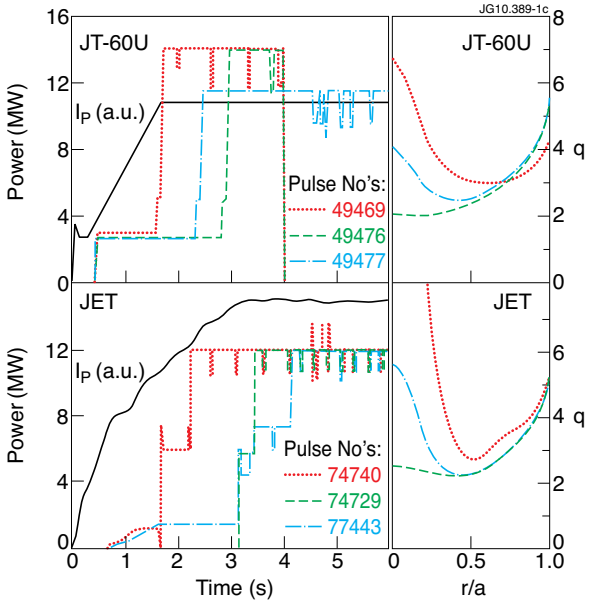

Figure 1: JT-60U (top) and JET (bottom) scenarios with different NBI power waveform. Three different target q-profiles measured at the start of the main heating phase by MSE diagnostic. The time base of JT-60U and JET data has been adjusted such that the start of the current ramp-up is at t = 0s.

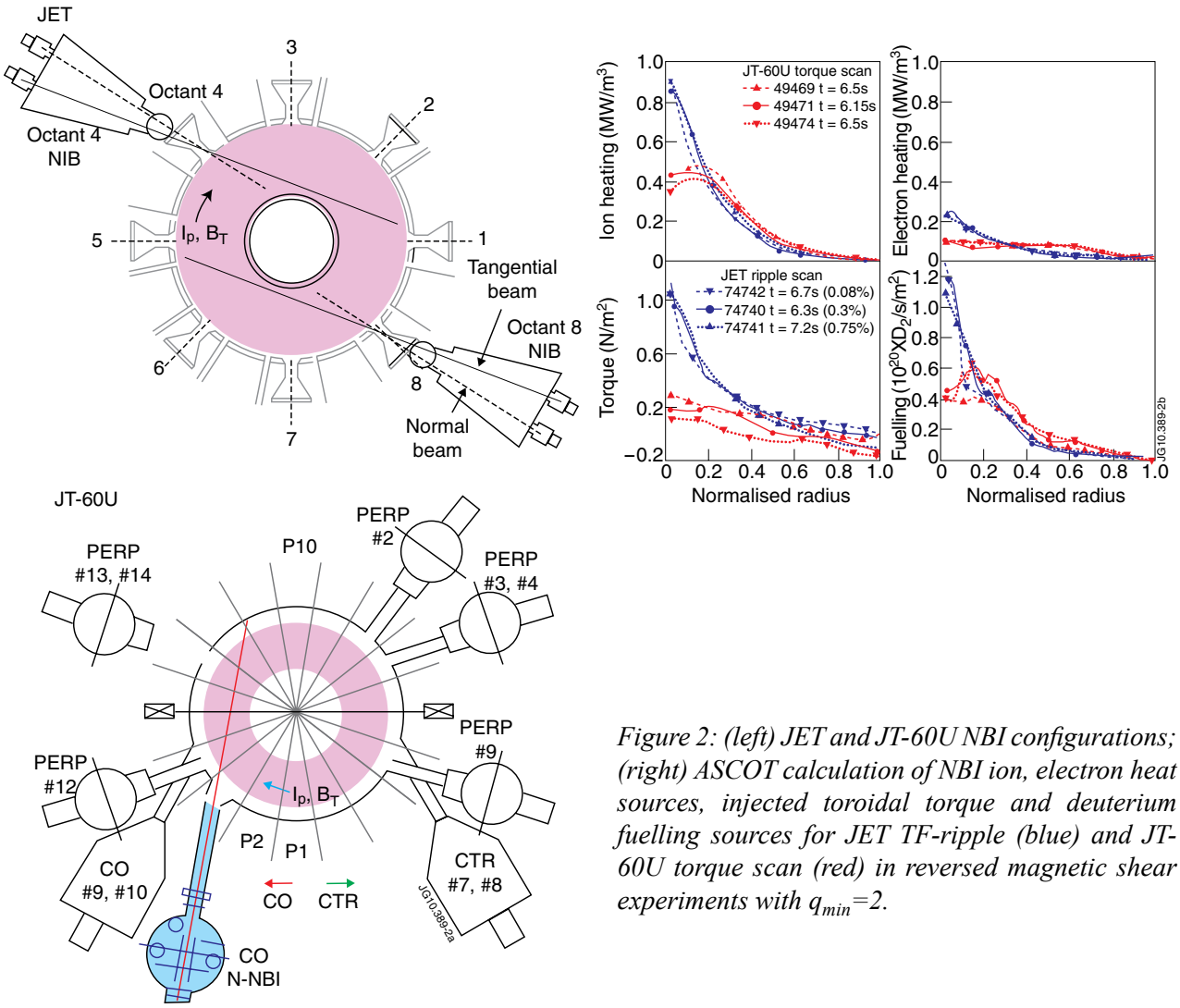

Figure 2: (left) JET and JT-60U NBI configurations; (right) ASCOT calculation of NBI ion, electron heat sources, injected toroidal torque and deuterium fuelling sources for JET TF-ripple (blue) and JT-60U torque scan (red) in reversed magnetic shear experiments with q_{min}=2.

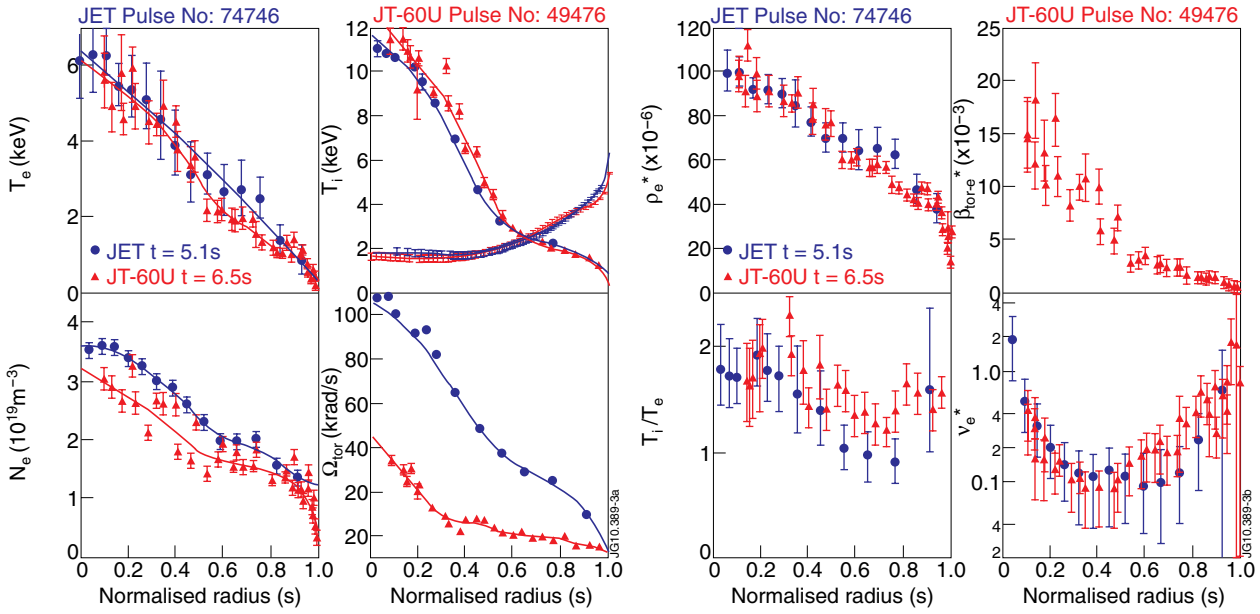

Figure 3: Optimised magnetic shear experiments with $q_o \sim 2$ for JET (blue) and JT-60U (red):(top-left) T_e, T_i, q, n_e, toroidal angular profiles; (top right) profiles of the dimensionless parameters.

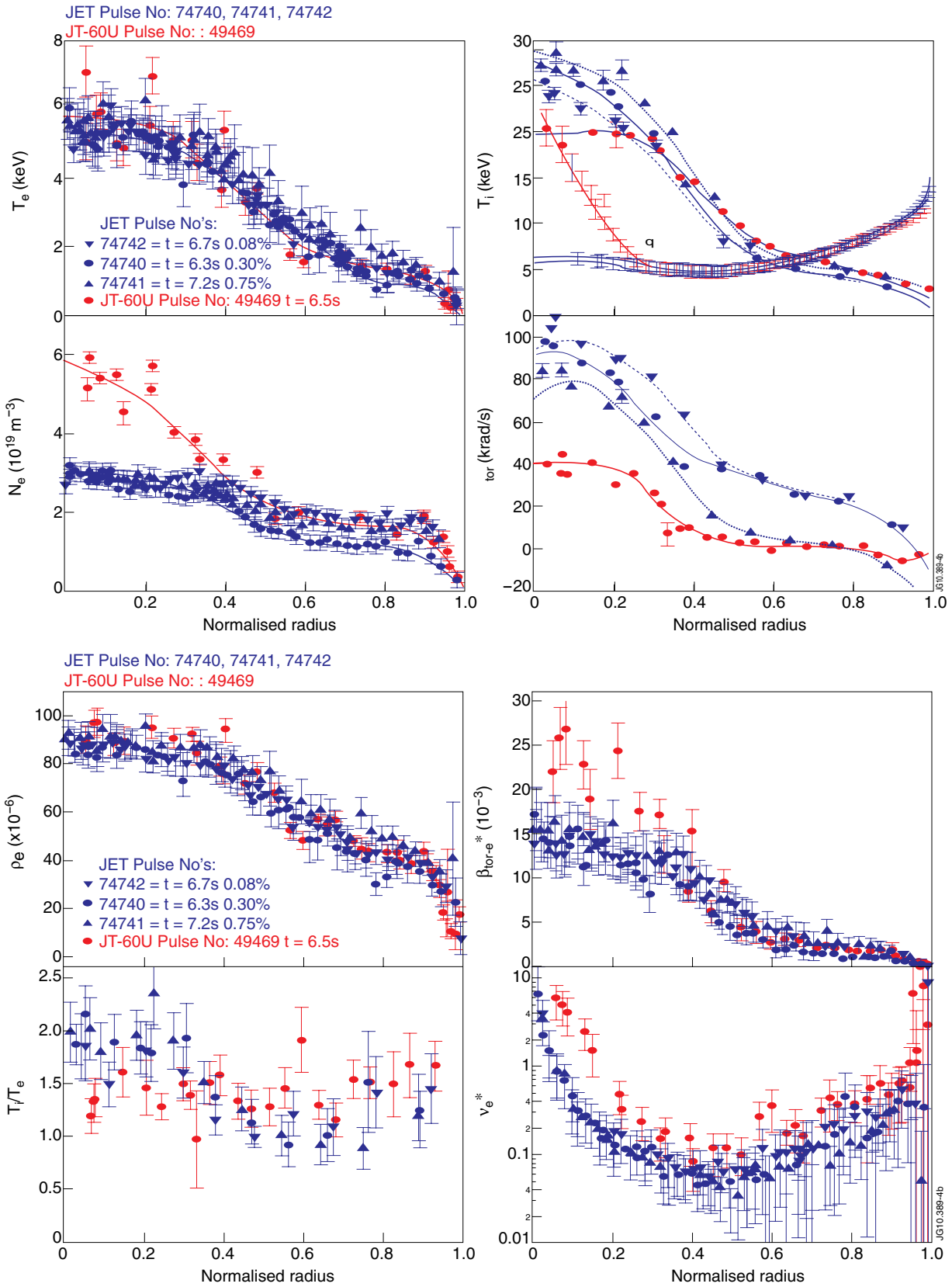

Figure 4: Reversed shear experiments with q_{min}~2 for JET TF ripple scan (blue) and JT-60U (red):(left) T_e, T_i, safety factor, n_e, toroidal angular profiles; (right) profiles of the dimensionless parameters, ρ_e, β and T_e/T_i, ν_e* . Profiles shown at the time of the fully developed ITB phase.*

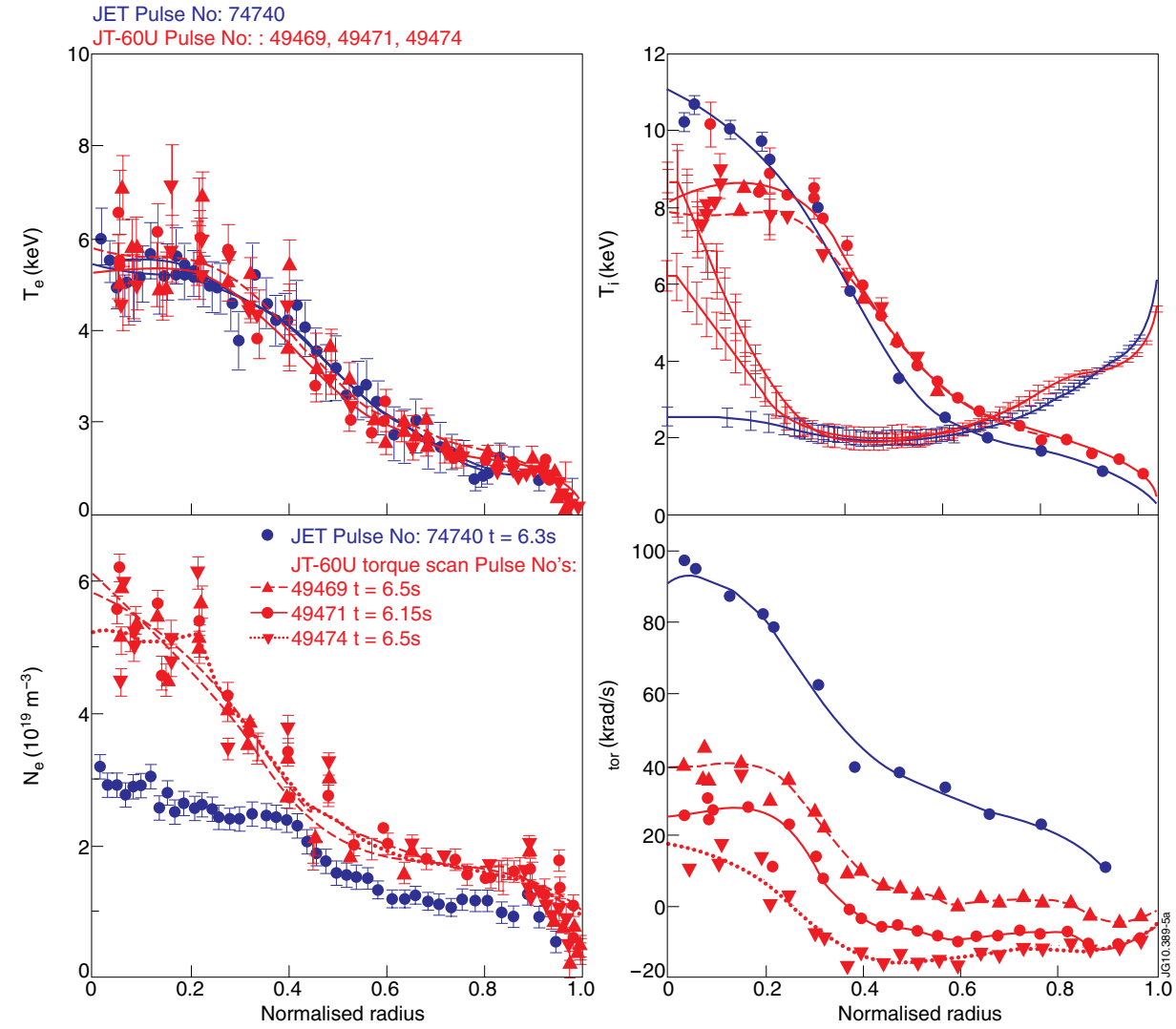

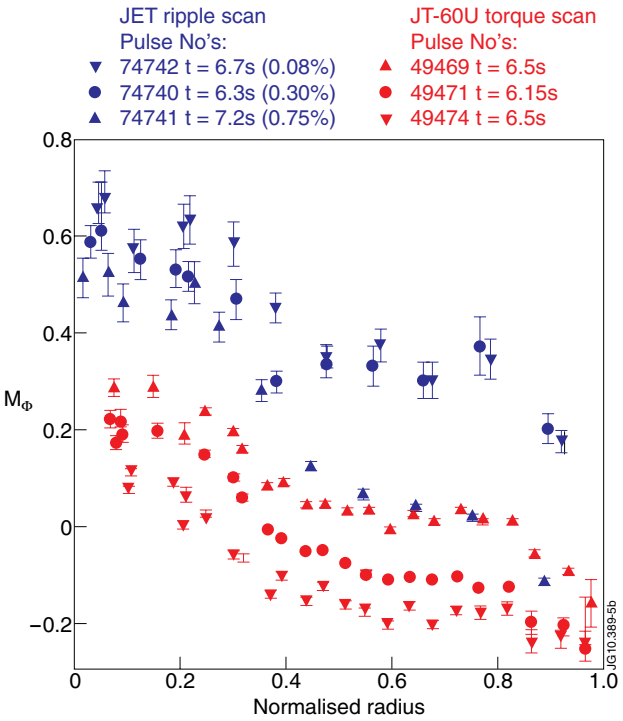

Figure 5: Reversed shear experiments with q_{min} ~ 2 for JET with $\delta_{TF} = 0.3\%$ (blue) and JT-60U injected torque scan (red):(left) T_e, T_i, safety factor, n_e, toroidal angular profiles; (right) profiles of the dimensionless toroidal Mach number for the JT-60U injected torque scan (red) and JET TF ripple scan. Profiles shown at the time of the fully developed ITB phase.

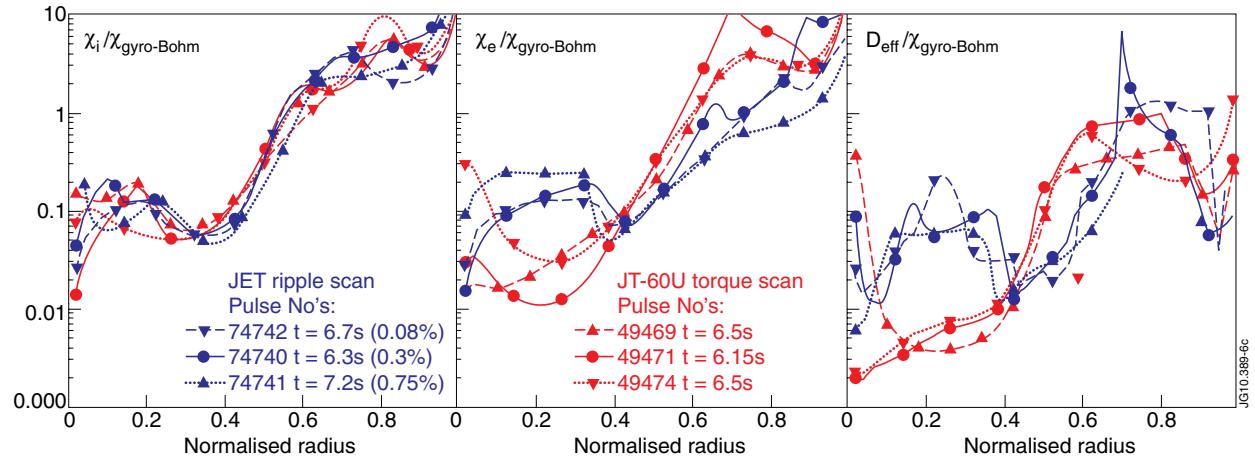

Figure 6: Reversed shear experiments with $q_{min} \sim 2$ for JET TF ripple (blue) and JT-60U torque scans (red): thermal ion, electron, effective electron particle diffusivities normalized to gyro-Bohm level.

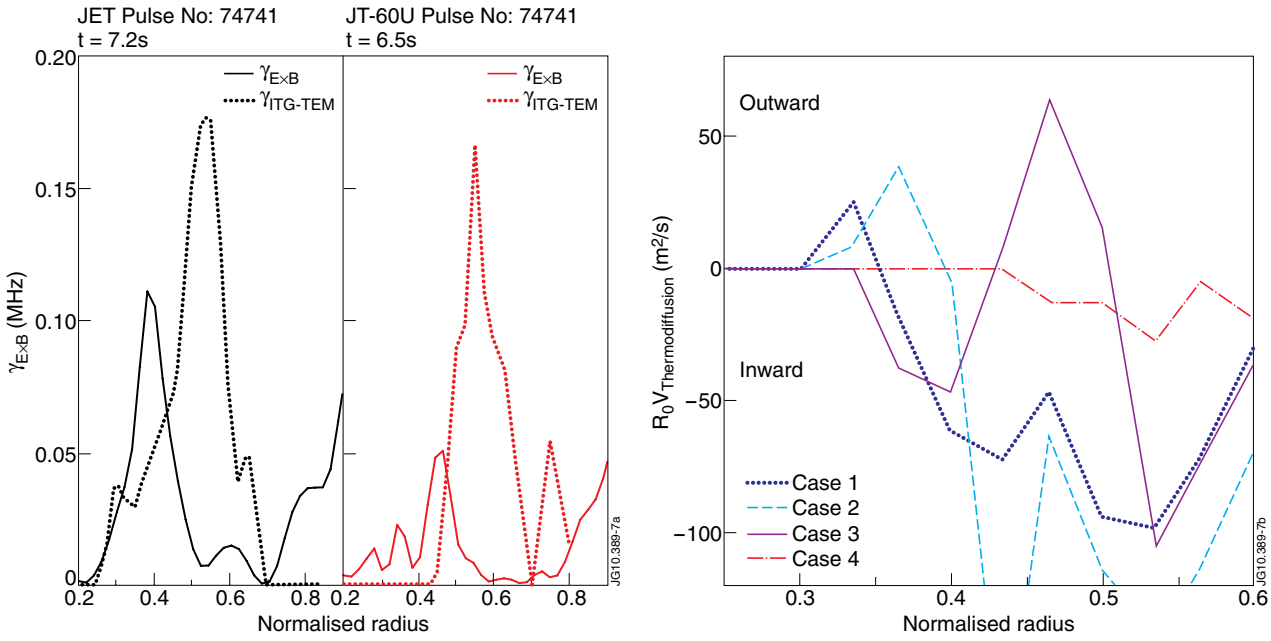

Figure 7: (left) Reversed shear JET Pulse No: 74741 and JT-60U Pulse No: 49469; (full line) $\gamma_{E\times B}$, (dashed line) $\gamma_{ITG\text{-}TEM}$ ($k_\perp \rho_e < 2$) calculated with QuaLiKiz. (right) QuaLiKiz calculation of the anomalous electron thermodiffusion, $R_o V_{thermodiffusion}$, for JT-60U: (case 1)closed square, weak shear discharge (Pulse No:49476, t=6.5s); (case 2) closed circles, the same case as (1) but $\nabla T_e/T_e$ multiplied by two; (case 3) closed triangle, the same case as (1) but the q-profile is taken from the reversed shear discharge (Pulse No:49469, t=6.5s); (case 4)red line, the reversed shear discharge (Pulse No:49469, t=6.5s).